

# Designable Optical Polyesters via Alternating Copolymerization of Benzaldehyde-derived Cyclic Carbonates and Phthalic Anhydride

Xue-Lin Song<sup>a,b</sup>, Shun-Jie Liu<sup>a,b\*</sup>, and Xian-Hong Wang<sup>a,b\*</sup><sup>a</sup> State Key Laboratory of Polymer Science and Technology, Changchun Institute of Applied Chemistry, Chinese Academy of Sciences, Changchun 130022, China<sup>b</sup> School of Applied Chemistry and Engineering, University of Science and Technology of China, Hefei 230026, China Electronic Supplementary Information

**Abstract** We report a platform-based approach for designing of aromatic polyesters with customizable optical properties. By employing a series of benzaldehyde-derived cyclic carbonate monomers, we performed ring-opening alternating copolymerization with phthalic anhydride to yield structurally regular polyesters featuring diverse substituents. All monomers underwent smooth copolymerization, producing polymers with controlled molecular weights ( $M_n=21-45$  kDa) and narrow dispersity ( $D=1.04-1.28$ ). Thermal analysis revealed decomposition temperatures above 280 °C and glass transition temperatures exceeding 90 °C, ensuring robust thermal stability. The resulting polyesters showed excellent visible-light transparency, with transmittance greater than 92% between 400–600 nm. Systematic modification of aromatic substituents enabled continuous tuning of refractive indices from 1.563 to 1.622, alongside Abbe numbers ranging from 30.9 to 45.1, highlighting the significant impact of electronic polarizability on optical performance. This work establishes a unified molecular design platform for creating high-performance optical polyesters with predictable and tunable refractive and dispersive properties.

**Keywords** Optical polyester; Cyclic carbonate; Designable properties

**Citation:** Song, X. L.; Liu, S. J.; Wang, X. H. Designable optical polyesters via alternating copolymerization of benzaldehyde-derived cyclic carbonates and phthalic anhydride. *Chinese J. Polym. Sci.* <https://doi.org/10.1007/s10118-026-3630-9>

## INTRODUCTION

As optical devices advance toward greater integration and an expanding range of applications, optical resins must be designed to satisfy multiple performance criteria, rather than being optimized for a single property.<sup>[1,2]</sup> Practical applications typically demand access to different application-relevant property windows defined by combinations of adjustable refractive index, dispersion, optical transparency, and thermal stability.<sup>[3-5]</sup> Achieving this level of controllability requires material systems whose properties can be tuned in a rational and predictable manner.<sup>[6]</sup> In this regard, molecular-level polymer design, through precise control of the monomer structure, provides a fundamentally different strategy from the traditional empirical formulation or simple blending, enabling systematic access to application-specific optical property windows.<sup>[7,8]</sup>

The optical properties of polymers can be precisely tuned through molecular-level structural design, and considerable progress has been made in this field. Previous studies have shown that the systematic modulation of optical properties, such as refractive index, dispersion, and transparency, can be realized by tailoring monomer structures, backbone architectures, side-chain configurations, and the spatial arrangement

of repeating units. Consequently, a variety of structural motifs with high electronic polarizability, including aromatic rings,<sup>[9-11]</sup> sulfur-containing groups,<sup>[12-14]</sup> and halogenated units,<sup>[15]</sup> have been widely incorporated into optical-polymer systems. Among these motifs, aromatic rings are particularly attractive because of their versatile substitution patterns and strong contribution to the molecular polarizability.<sup>[9,16]</sup> From a structural design perspective, aromatic units also provide an effective way to translate substituent-level electronic effects into polymer-level optical responses, provided that they can be incorporated in a well-defined and structurally anchored manner. In this context, our previous studies demonstrated that ring-opening alternating copolymerization of cyclic carbonates and anhydrides affords structurally regular polyesters with precisely defined repeating units.<sup>[17,18]</sup> In these systems, aromatic moieties are integrally embedded within the repeating-unit architecture, creating a well-defined chemical environment in which aromatic structures are consistently positioned relative to the polymer backbone. These alternating polyesters exhibit favorable optical characteristics, underscoring the potential of carbonate-anhydride copolymerization as a robust platform for optical resin design. However, despite these advantages, modifying the existing cyclic carbonate monomers, particularly tyrene carbonate, directly and systematically on the aromatic ring while preserving the carbonate framework, remains synthetically challenging.<sup>[19]</sup> This limitation hinders precise control over substituent electronics and their spatial anchoring within the

\* Corresponding authors, E-mail: [sjliu@ciac.ac.cn](mailto:sjliu@ciac.ac.cn) (S.J.L.)

E-mail: [xhwang@ciac.ac.cn](mailto:xhwang@ciac.ac.cn) (X.H.W.)

Received January 22, 2026; Accepted February 21, 2026; Published online April 16, 2026

polymer structure, thereby restricting the systematic correlation between substituent effects and optical performance, and narrowing the accessible optical property windows within a unified polymer framework.

Building on this foundation, we aimed to overcome the limitations of the monomer in designing aromatic cyclic carbonates while retaining the structural precision achieved through carbonate-anhydride alternating copolymerization. In this context, benzaldehydes represent strategically advantageous starting points for monomer development. From a supply side perspective, benzaldehyde derivatives are commercially abundant and contain a broad range of electronically diverse substituents. From a design-demand perspective, the aldehyde functionality enables efficient and programmable transformation into cyclic carbonate monomers *via* a simple one-pot, two-step protocol while preserving precise control over aromatic substitution patterns. The incorporation of these benzaldehyde-derived cyclic carbonates into ring-opening alternating copolymerization with anhydrides enables the structural embedding of substituted aromatic units within well-defined repeating units of the resulting polyesters. In this architecture, the aromatic motif is simultaneously integrated into the backbone environment and is presented as a pendant structural element within each repeat unit (Scheme 1). This dual anchoring strategy establishes a direct and unambiguous link between the monomer design and polymer architecture, allowing substituent-level electronic effects to be systematically translated into tunable optical properties.<sup>[20]</sup> Consequently, this platform enables the construction of aromatic polyesters that span distinct refractive indices and dispersion windows within a unified and predictable molecular framework.

## EXPERIMENTAL

### Materials

All moisture/oxygen-sensitive reactions were carried out in a glove box or using standard Schlenk techniques under dry nitrogen. Phthalic anhydride (PA) was sublimed three times under reduced pressure and then stored in a glovebox for further

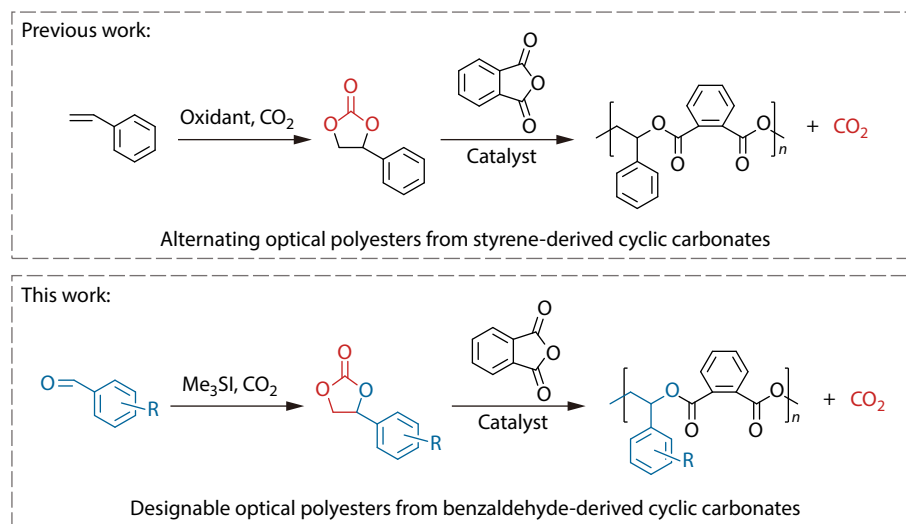
use. Bis(triphenylphosphoranylidene)ammonium chloride (PPN-Cl), sodium benzoate, potassium hydroxide, trimethylsulfonium iodide, 3,5-dimethoxybenzaldehyde, 4-bromobenzaldehyde, 4-cyanobenzaldehyde, 4-methylsulphonyl benzaldehyde, 1-naphthaldehyde and other reagents were purchased from Energy Chemical and used without further purification. The synthesized catalysts (PPNOBz) and monomers (**M1–M5**) were further purified *via* recrystallization and dried under vacuum.

### Characterization

Nuclear magnetic resonance (NMR) spectra were recorded on an ARX-500 spectrometer at ambient temperature in deuterated chloroform ( $\text{CDCl}_3$ ), with tetramethylsilane (TMS) as the internal reference. Gel permeation chromatography (GPC) was performed at 35 °C relative to a polystyrene standard on a Waters e2695 GPC instrument with dichloromethane as the eluent at a flow rate of 1.0 mL·min<sup>-1</sup>. Thermogravimetric analysis (TGA) was performed using a Mettler-Toledo TGA 1 instrument. Powder polymer samples were heated from 30 °C to 500 °C at a rate of 10 °C·min<sup>-1</sup> under nitrogen flow (100 mL·min<sup>-1</sup>). Differential scanning calorimetry (DSC) of the polymer samples was performed using a Mettler Toledo Polymer DSC instrument equipped with a Julabo chiller and autosampler. Typical DSC experiments were conducted in crimped aluminum pans at a heating rate of 10 °C·min<sup>-1</sup> from 0 °C to 200 °C under a blanket of dry nitrogen. Data were processed using the StarE software. UV-Vis spectra were obtained on a UV2600 spectrophotometer with samples spin-coated on a quartz wafer from a chloroform solution (10 mg·mL<sup>-1</sup>) at a rotating speed of 1000 r·min<sup>-1</sup>. All measurements were performed between 400 and 800 nm. Refractive index measurements were performed using a spectroscopic ellipsometer with samples spin-coated on a silica wafer from a chloroform solution (10 mg·mL<sup>-1</sup>) at a rotating speed of 1000 r·min<sup>-1</sup>.

### Catalyst Synthesis

PPNOBz was prepared according to literature procedures (yield, 80%).<sup>[21]</sup> <sup>1</sup>H-NMR (500 MHz,  $\text{CDCl}_3$ ,  $\delta$ , ppm): 8.18–8.15 (m, 2H), 7.66–7.59 (m, 6H), 7.47–7.36 (m, 24H), 7.33–7.18 (m, 24H).



**Scheme 1** Synthetic route to alternating optical polyesters.

## Monomer Synthesis

### Synthesis of **M1**

In a 75 mL stainless-steel autoclave, 3,5-dimethoxybenzaldehyde (25 mmol) was dissolved in acetonitrile (50 mL). Trimethylsulfonium iodide (25 mmol), potassium hydroxide (50 mmol), and water (0.1 mL) were then added, and the reaction mixture was heated at 80 °C for 4 h. The autoclave was then charged with CO<sub>2</sub> at a pressure of 4 MPa and heated to 100 °C for 24 h. After cooling to room temperature and carefully releasing CO<sub>2</sub>, the reaction mixture was transferred, and the solvent was removed under reduced pressure. The crude product was purified by flash column chromatography on silica gel using dichloromethane as the eluent, followed by recrystallization thrice to afford **M1** as a white solid (yield: 85%). <sup>1</sup>H-NMR (500 MHz, CDCl<sub>3</sub>, δ, ppm): 6.46 (s, 3H), 5.60 (t, 1H), 4.77 (t, 1H), 4.30 (dd, 1H), 3.80 (s, 6H); <sup>13</sup>C-NMR (100 MHz, CDCl<sub>3</sub>, δ, ppm): 161.66, 154.89, 138.31, 103.57, 101.34, 77.89, 71.23, 55.66.

### Synthesis of **M2**

A procedure similar to that described for **M1** was employed, using 4-bromobenzaldehyde as the starting material (yield: 85%). <sup>1</sup>H-NMR (500 MHz, CDCl<sub>3</sub>, δ, ppm): 7.60–7.57 (m, 2H), 7.25–7.23 (m, 2H), 5.64 (t, 1H), 4.80 (t, 1H), 4.30 (dd, 1H); <sup>13</sup>C-NMR (100 MHz, CDCl<sub>3</sub>, δ, ppm): 154.60, 134.98, 132.65, 127.60, 124.10, 77.37, 71.05.

### Synthesis of **M3**

A procedure similar to that described for **M1** was employed, using 4-cyanobenzaldehyde as the starting material (yield: 85%). <sup>1</sup>H-NMR (500 MHz, CDCl<sub>3</sub>, δ, ppm): 7.77–7.75 (m, 2H), 7.50–7.49 (m, 2H), 5.74 (t, 1H), 4.87 (t, 1H), 4.30 (dd, 1H); <sup>13</sup>C-NMR (100 MHz, CDCl<sub>3</sub>, δ, ppm): 154.21, 141.10, 133.25, 126.42, 118.01, 113.91, 76.71, 70.80.

### Synthesis of **M4**

A procedure similar to that described for **M1** was employed, using 4-methylsulphonyl benzaldehyde as the starting material (yield: 70%). <sup>1</sup>H-NMR (500 MHz, CDCl<sub>3</sub>, δ, ppm): 8.04–8.03 (m, 2H), 7.59–7.58 (m, 2H), 5.78 (t, 1H), 4.89 (t, 1H), 4.32 (dd, 1H), 3.07 (s, 3H); <sup>13</sup>C-NMR (100 MHz, CDCl<sub>3</sub>, δ, ppm): 154.29, 142.09, 141.96, 128.60, 126.72, 76.73, 70.86, 44.54.

### Synthesis of **M5**

A procedure similar to that described for **M1** was employed, using 1-naphthaldehyde as the starting material (yield: 74%). <sup>1</sup>H-NMR (500 MHz, CDCl<sub>3</sub>, δ, ppm): 7.97–7.90 (m, 2H), 7.69–7.53 (m, 5H), 6.42 (t, 1H), 5.06 (t, 1H), 4.39 (dd, 1H); <sup>13</sup>C-NMR (100 MHz, CDCl<sub>3</sub>, δ, ppm): 154.93, 133.96, 131.87, 129.89, 129.62, 129.35, 127.35, 126.51, 125.64, 122.48, 121.67, 75.68, 70.92.

## Ring-opening Alternating Polymerization of Aromatic Cyclic Carbonates (**M1–M5**) and PA

Ring-opening alternating copolymerization (ROAC) of aromatic cyclic carbonates (**M1–M5**) and PA was conducted in a 10 mL stainless-steel autoclave equipped with a magnetic stirrer. The autoclave was charged with predetermined amounts of monomers and catalyst in a glovebox, sealed, and immersed in a preheated oil bath. After the desired polymerization time, the autoclave was removed from the oil bath and cooled to room temperature. The resulting crude polymer was directly used for <sup>1</sup>H-NMR analysis to determine the monomer conversion. Subsequently, the crude product was fully dissolved in dichloromethane and precipitated by dropwise addition of methanol. This dissolution-precipitation process was repeated three times. The purified polymer was dried in a vacuum oven at 60 °C for 12 h and used for further characterization.

## RESULTS AND DISCUSSION

### Monomer Design

At the monomer design level, a unified synthetic strategy utilizing substituted benzaldehydes has been employed to produce aromatic cyclic carbonate monomers. By slightly modifying the literature procedure,<sup>[22]</sup> a series of substituted aromatic cyclic carbonates was synthesized *via* a one-pot, two-step process, thereby overcoming the limited substrate scope associated with traditional methods based on phenylethylene glycol<sup>[23,24]</sup> or styrene<sup>[25]</sup> derivatives (Fig. 1). This benzaldehyde-based route offers two practical advantages: first, it leverages the broad commercial availability and mature industrial supply of substituted benzaldehydes, making them more accessible and cost-effective than specialized diols or epoxides; second, their widespread use in fine chemicals and pharmaceuticals provides a versatile platform for modular functionalization and systematic material development. Within this framework, aryl substituents were rationally selected to explore their effects on the monomer structure and the properties of the resulting polyesters. Meta-dimethoxy substitution was introduced to adjust the local steric environment and conformational flexibility around the aromatic ring, while bromine,<sup>[9]</sup> cyano<sup>[26]</sup> and methanesulfonyl<sup>[27]</sup> groups were incorporated as highly polarizable or strongly electron-withdrawing units with the potential to affect the molar refractivity. In addition, extending the core from benzene to naphthalene<sup>[28]</sup> enabled the examination of how increased aromatic conjugation might influence polymerization behavior and material characteristics. Although this study focuses on these derivatives, the strategy could, in principle, accommodate other compatible substrates, including het-

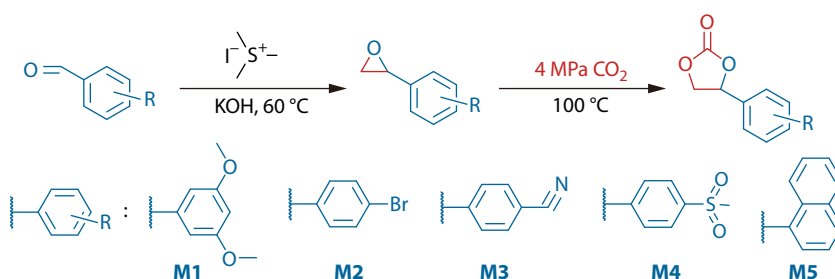


Fig. 1 Synthetic route to **M1–M5**.

eroaromatics, provided that they do not interfere with the anionic propagating species. Collectively, this feedstock-driven approach furnishes a structurally diverse and internally comparable monomer set, providing a versatile platform for systematic structure-property investigations of aromatic polyesters.

### Ring-opening Alternating Polymerization of Aromatic Cyclic Carbonates (M1–M5) and PA

The polymerization behavior of these monomers was examined under identical conditions following our established procedure ([M]/PA/PPNOBZ = 200/200/1, 180 °C; Table 1).<sup>[17]</sup> The use of the metal-free organic catalyst PPNOBz offers significant advantages for optical polymer synthesis because it prevents metal-induced coloration and enables the production of colorless polyesters.

Due to differences in the electronic properties and steric profiles of the substituents, all monomers underwent smooth alternating copolymerization, affording polyesters with relatively narrow molecular weight distributions (1.04–1.28) and unimodal GPC traces (Fig. 2a). This consistent behavior across the monomer series indicates that the polymerization system is robust and highly reproducible and that the introduction of diverse substituents does not compromise the alternating selectivity.<sup>[29]</sup>

A detailed comparison of the polymerization rate and molecular weight revealed that substituent effects extend beyond the initial nucleophilic ring-opening step and influence the behavior of the alkoxide species during chain growth.<sup>[30,31]</sup> As a result, turnover frequency (TOF) and number-average molecular weight ( $M_n$ ) should be viewed as integrated descriptors of the overall polymerization process rather than as direct indicators of isolated electronic or steric effects (Figs. 2b and 2c).<sup>[32,33]</sup> Notably, under otherwise identical conditions, polymerization rate and molecular weight do not correlate, suggesting that different stages of the copolymerization are governed by different structural factors.<sup>[34]</sup>

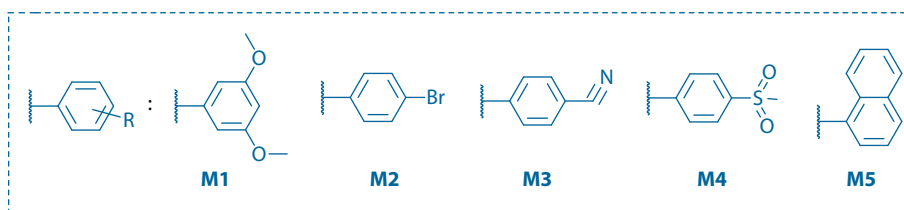
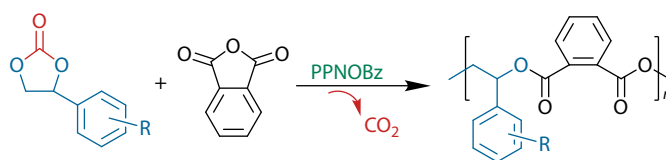
Weakly electron-donating dimethoxy and weakly electron-

withdrawing bromo substituents afford the highest molecular weights ( $M_n$ =44.6 and 37.2 kDa, respectively) with moderate TOFs of 621 and 525 h<sup>-1</sup>, respectively. This suggests that mild electronic effects do not significantly alter the carbonate ring-opening kinetics but promote sustained chain growth (Table 1, entries 1 and 2).<sup>[35,36]</sup> In contrast, the strongly electron-withdrawing cyano substituent leads to the fastest polymerization (TOF=860 h<sup>-1</sup>) but produces polymers with substantially lower molecular weight ( $M_n$ =21.4 kDa, Table 1, entry 3). This behavior aligns with rapid initiation driven by increased carbonate electrophilicity,<sup>[37]</sup> coupled with reduced propagation efficiency due to stabilization of the alkoxide chain end, which likely encourages chain transfer or reversible processes.

The methanesulfonyl-substituted system exhibits a decreased TOF (486 h<sup>-1</sup>) and  $M_n$  (23.3 kDa), which is consistent with the experimentally observed poor solubility of both the monomer and resulting polymer (Table 1, entry 4).<sup>[38]</sup> Similarly, the naphthyl-substituted monomer displayed a relatively low polymerization rate and moderate molecular weight (TOF=436 h<sup>-1</sup>,  $M_n$ =26.2 kDa), indicating that the increased steric hindrance and limited conformational flexibility outweigh the potential advantages of enhanced aromatic polarizability (Table 1, entry 5).<sup>[39]</sup> The slightly higher dispersity of **P5** ( $\mathcal{D}$ =1.28) compared to other polymers can be attributed to the increased steric hindrance of the naphthyl group, which could reduce the monomer insertion rate during the propagation step. Overall, the effects of substituents are primarily reflected in variations in polymerization outcomes, such as molecular weight and efficiency, while the robustness of alternating copolymerization remains consistent throughout the series. Rather than establishing a predictive structure-reactivity relationship, these findings provide a qualitative reference for understanding substituent effects in aromatic cyclic carbonate-based polyester systems.

The regioselective ring opening of cyclic carbonates was

**Table 1** ROAC of aromatic cyclic carbonates (**M1–M5**) and PA.<sup>a</sup>



Entry	Monomer	<i>t</i> (min)	TOF <sup>b</sup> (h <sup>-1</sup> )	Conv. [M] <sup>c</sup> (%)	Conv. PA <sup>c</sup> (%)	$M_n^d$ (kDa)	$\mathcal{D}^d$
1	( <b>P1</b> ) <b>M1</b> /PA	17	621	88	90	44.6	1.04
2	( <b>P2</b> ) <b>M2</b> /PA	21	525	92	93	37.2	1.13
3	( <b>P3</b> ) <b>M3</b> /PA	11	862	79	82	21.4	1.17
4	( <b>P4</b> ) <b>M4</b> /PA	20	486	81	83	23.3	1.09
5	( <b>P5</b> ) <b>M5</b> /PA	25	436	91	ND	26.2	1.28

<sup>a</sup> Reaction conditions: [M]/PA/PPNOBZ = 200/200/1, [M] = 5 mmol, in a pre-dried 10 mL autoclave, in bulk, *T*=180 °C; <sup>b</sup> Turnover frequency (TOF) = mol of product (polyester)/mol of catalyst per hour; <sup>c</sup> Calculated by <sup>1</sup>H-NMR; <sup>d</sup> Determined by GPC in CH<sub>2</sub>Cl<sub>2</sub> at 35 °C relative to the polystyrene standard.

examined using a model reaction of [M]/PPNOBz/benzoic acid = 20/1/20 at 180 °C for 10 min (Table 2, Figs. S22–S26 in the electronic supplementary information, ESI). Benzoic acid (HOBz) served as a proton source to capture ring-opened intermediates and prevent the formation of anionic species other than OBz.<sup>[40]</sup> This small-molecule reaction provides a convenient model to examine the preferred site of OBz attack on **M1–M5** and to approximate nucleophilic attack by PA-generated carboxylate chain ends during copolymerization. For dimethoxy- and bromo-substituted systems, the CH<sub>2</sub>/CH ratios remained close to 2/1, indicating that regioselectivity is primarily governed by steric hindrance when the electronic effects are modest. In contrast, the methanesulfonyl- and naphthyl-substituted systems show increased at-

tack at the methine carbon, with CH<sub>2</sub>/CH = 1.29/1 and 1.56/1, respectively, indicating a greater influence of electronic factors on ring opening. Notably, the strongly electron-withdrawing cyano-substituted carbonates exhibit the highest CH<sub>2</sub>/CH ratio (2.57/1). This pronounced electron-withdrawing effect at both the methylene and methine positions significantly activates the carbonate ring electronically, rendering the monomer more susceptible to nucleophilic attack. This enhanced electrophilicity is also reflected in its substantially higher apparent ring-opening activity during copolymerization compared to other monomers. Collectively, the regioselectivity trends observed in this small-molecule model offer valuable structural insights into the influence of aromatic substituents on both the ring-opening behavior and the re-

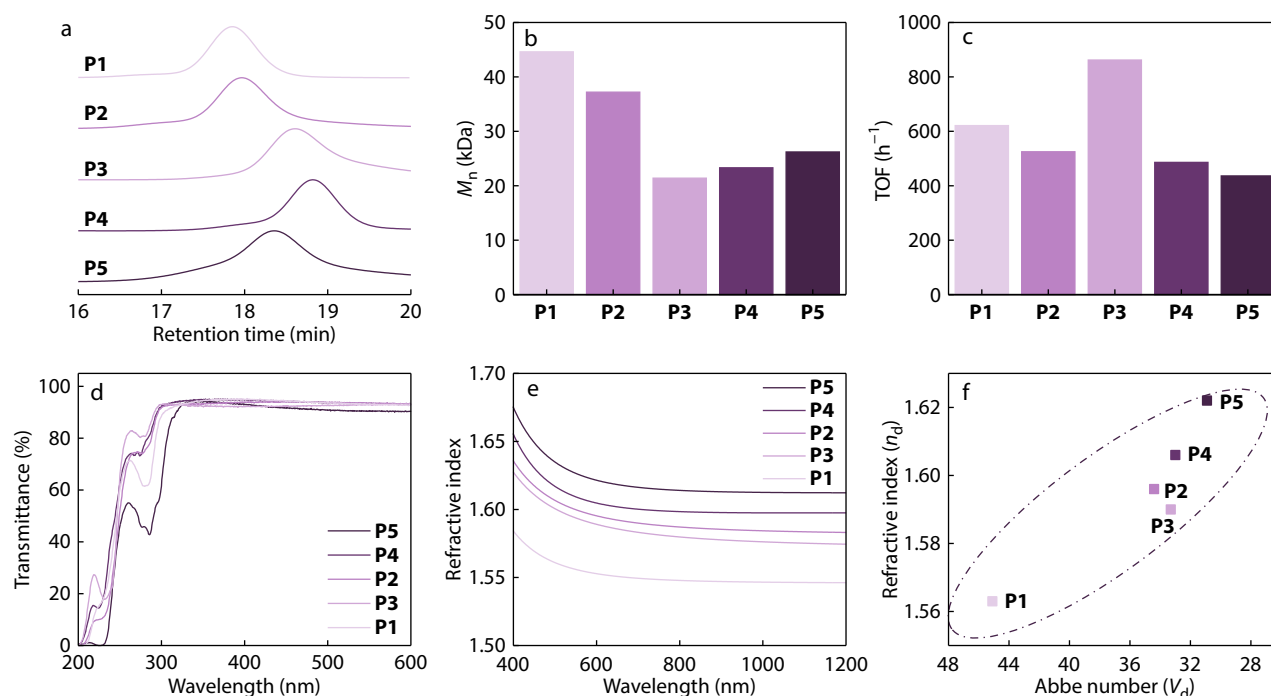
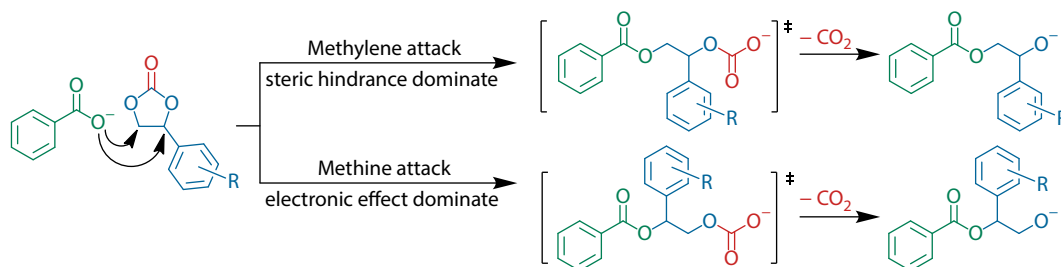


**Fig. 2** (a) GPC curves of **P1–P5** in Table 1; Comparison of (b)  $M_{n,GPC}$  and (c) TOF of **P1–P5**; (d) UV-Vis transmittance spectra of **P1–P5**; (e) Wavelength-dependent refractive indices of **P1–P5** determined by spectroscopic ellipsometer; (f) **P1–P5** in the  $n_d$ - $V_d$  diagram.

**Table 2** Substituent effects on regioselectivity of cyclic carbonate ring-opening.



Entry	Monomer	$\delta(-CH_2-)^a$ (ppm)	$\delta(-CH-)^a$ (ppm)	Methylene/methine attack ratio <sup>b</sup>
1	<b>M1</b>	77.89	71.23	1.97
2	<b>M2</b>	77.37	71.05	1.96
3	<b>M3</b>	76.71	70.80	2.57
4	<b>M4</b>	76.73	70.86	1.29
5	<b>M5</b>	75.68	70.92	1.56

<sup>a</sup> Determined by <sup>13</sup>C-NMR; <sup>b</sup> Calculated by <sup>1</sup>H-NMR.

**Table 3** The properties of **P1–P5**.

Entry	Sample	$M_n^a$ (kDa)	PDI <sup>a</sup>	$T_d^b$ (°C)	$T_g^c$ (°C)	$n_d^d$	$V_d^d$
1	<b>P1</b>	44.6	1.04	312.72	91.32	1.563	45.1
2	<b>P2</b>	37.2	1.13	302.67	115.17	1.596	34.4
3	<b>P3</b>	21.4	1.17	321.33	141.01	1.590	33.3
4	<b>P4</b>	23.3	1.09	314.50	154.68	1.606	33.0
5	<b>P5</b>	26.2	1.28	282.12	124.77	1.622	30.9

<sup>a</sup> Determined by GPC in  $\text{CH}_2\text{Cl}_2$  at 35 °C relative to the polystyrene standard; <sup>b</sup> Determined using TGA; <sup>c</sup> Determined by DSC; <sup>d</sup> Determined using a spectroscopic ellipsometer.

sulting polymerization outcomes.<sup>[22,41]</sup>

### Thermal Properties

Thermogravimetric analysis (TGA) and differential scanning calorimetry (DSC) were performed to assess the thermal robustness of the synthesized polyesters (Figs. S27–S36 in ESI and Table 3). The dimethoxy-, bromo-, cyano-, and methylsulfonyl-substituted polymers (**P1–P4**) all exhibit decomposition temperatures ( $T_{d5\%wt}$ ) above 300 °C, indicating excellent thermal stability. The naphthyl-substituted polymer (**P5**) displays a slightly lower  $T_{d5\%wt}$  of 282 °C, likely due to the bulky naphthyl group increasing the local free volume, which modestly reduces the thermal stability. Nonetheless, this decomposition temperature is sufficient for the typical processing and usage of optical resins.<sup>[42]</sup> DSC measurements reveal a clear trend in glass transition behavior: **P1** has a  $T_g$  of 91.32 °C, while **P2–P5** all display  $T_g$  values exceeding 100 °C, indicating dimensional and optical stability at elevated operating temperatures. Overall, despite minor variations in the thermal properties of the polymers, all the materials demonstrated adequate thermal stability and glass transition temperatures, which are suitable for optical resin applications. These results confirm that the current monomer and polymer design strategy provides robust thermal performance, while maintaining a primary focus on tuning the optical properties.

### Transparency

Optical transparency is essential for optical polymers designed for refractive applications because a high refractive index is only valuable when paired with adequate light transmission in the visible region. To assess this, the optical transparency of the synthesized polymers was measured using UV-Vis spectroscopy on solution-cast films (100  $\mu\text{m}$  thick). As shown in Fig. 2(d), all the polymers exhibit excellent transparency in the visible range, with transmittance values exceeding 92% across 400–600 nm, indicating minimal optical loss under practical conditions. In the ultraviolet region, absorption features appear mainly between 200 and 300 nm, which are attributed to the  $\pi\text{-}\pi^*$  transitions associated with the aromatic units.<sup>[43]</sup> Importantly, no low-energy electronic transitions extended into the visible region, resulting in a sharp absorption edge and high transparency above ca. 350 nm for all samples. Among the series, the naphthyl-substituted polymer displays relatively stronger and slightly red-shifted UV absorption, consistent with its extended aromatic conjugation; however, this absorption remains confined to the ultraviolet region and does not affect the visible-light transmission. Overall, these results confirm that all polymers maintain high optical clarity in the visible spectrum, providing the necessary optical window for further analysis of the refractive index and dispersion behavior.

### Refractive Index

The most widely accepted approach for designing optical poly-

mers is based on the Lorentz-Lorenz equation, which defines the fundamental relationship between the refractive index and intrinsic molecular properties. Eq. (1) expresses this relationship by relating the refractive index  $n$  in terms of the molar refractive index  $[R]$  and the molar volume  $V_0$ .

$$n = \sqrt{\frac{1 + 2[R]/V_0}{1 - [R]/V_0}} \quad (1)$$

Within this framework, the systematic modification of aryl substituents enables the continuous tuning of optical properties over a broad and practically relevant range.<sup>[44]</sup> All the polymers exhibit elevated refractive indices, showing clear substituent-dependent trends (Table 3 and Fig. 2e). **P1** has a relatively low refractive index ( $n_d=1.563$ ) and an Abbe number ( $V_d$ ) of 45.1, due to its increased molar volume. In contrast, **P2–P4** display higher refractive indices, ranging from 1.590 to 1.606, along with a reduced  $V_d$  value of approximately 33–34 (Fig. 2f). These results reflect the increasing contribution of the electronic polarizability to heavier or more polar substituents.

## CONCLUSIONS

In summary, we developed a versatile polymer design platform based on benzaldehyde-derived cyclic carbonates and phthalic anhydride, enabling the systematic tuning of the optical properties of aromatic polyesters. Alternating ring-opening copolymerization proceeded smoothly for all monomers, affording polymers with well-defined molecular weights and narrow dispersities, regardless of the substituent type. Substituent effects influenced polymerization kinetics, molecular weight, and regioselectivity: strongly electron-withdrawing groups accelerated initiation but limited chain growth, whereas bulky aromatic groups reduced the propagation efficiency. Thermal analysis confirmed decomposition temperatures above 280 °C and glass transition temperatures above 90 °C, ensuring dimensional and optical stabilities. Optical measurements revealed a high visible transparency (>92%) and a tunable refractive index window from 1.563 to 1.622, accompanied by trade-offs in the Abbe number (30.9–45.1) reflecting the impact of polarizability and conjugation. Collectively, these findings demonstrate that a systematic molecular-level structural design provides a predictable and effective route to high-performance optical polyesters, offering a platform for the future development of advanced optical resins with tailored property profiles.

## BIOGRAPHY

**2026 Rising Scholar:** Shun-Jie Liu received his Ph.D. degree from the Changchun Institute of Applied Chemistry (CIAC), Chinese Academy of Science in 2016 under the supervision of Prof.

Xian-Hong Wang. He conducted postdoctoral research at the Hong Kong University of Science and Technology with Prof. Ben Zhong Tang from 2016 to 2020. In 2021, he joined the State Key Laboratory of Polymer Science and Technology at CIAC and was promoted to full Professor. His research interests focus on CO<sub>2</sub>-based polymer materials.

### Conflict of Interests

Shun-Jie Liu is an editorial board member for *Chinese Journal of Polymer Science* and was not involved in the editorial review or the decision to publish this article. All authors declare that there are no competing interests.

### Electronic Supplementary Information

Electronic supplementary information (ESI) is available free of charge in the online version of this article at <http://doi.org/10.1007/s10118-026-3630-9>.

### Data Availability Statement

The data supporting the findings of this study are available from the corresponding author upon reasonable request.

### ACKNOWLEDGMENTS

This study was financially supported by the National Natural Science Foundation of China (Nos. 22271275, 52588201, and U25A20250).

### REFERENCES

- Kumar, R.; Kumar, N.; Chandel, S.; Tiwari, A.; Bag, A.; Ghorai, P. K.; Ghosh, N.; Shunmugam, R. Functional polymer material with efficient optical tunability. *ChemistrySelect* **2023**, *8*, e202302213.
- Wang, M. Y.; Zhang, Y.; Wang, D.; Yao, M.; Wang, Y. X.; Zhou, X. P.; Peng, H. Y.; Xie, X. L. Holographic polymer nanocomposites with high refractive index modulation by doping liquid crystal E6M. *Chinese J. Polym. Sci.* **2024**, *42*, 926–935.
- Badur, T.; Dams, C.; Hampp, N. High refractive index polymers by design. *Macromolecules* **2018**, *51*, 4220–4228.
- Mazumder, K.; Voit, B.; Banerjee, S. Recent Progress in sulfur-containing high refractive index polymers for optical applications. *ACS Omega* **2024**, *9*, 6253–6279.
- Higashihara, T.; Ueda, M. Recent progress in high refractive index polymers. *Macromolecules* **2015**, *48*, 1915–1929.
- Luo, M.; Zhang, X. H.; Du, B. Y.; Wang, Q.; Fan, Z. Q. Well-defined high refractive index poly(monothiocarbonate) with tunable abbe's numbers and glass-transition temperatures terpolymerization. *Polym. Chem.* **2015**, *6*, 4978–4983.
- Zhou, Y. T.; Zhu, Z. C.; Zhang, K.; Yang, B. Molecular Structure and Properties of sulfur-containing high refractive index polymer optical materials. *Macromol. Rapid Commun.* **2023**, *44*, 2300411.
- Zhao, Y. H.; Zhang, J.; Zhang, Y. X.; Cui, L.; Chi, Y.; Jian, Z. B. Advances in high refractive index cycloolefin-containing polymeric materials. *Macromolecules* **2025**, *58*, 10949–10962.
- Zhang, J.; Bai, T. W.; Liu, W. X.; Li, M. Z.; Zang, Q. G.; Ye, C.; Sun, J. Z.; Shi, Y. C.; Ling, J.; Qin, A.; Tang, B. Z. All-organic polymeric materials with high refractive index and excellent transparency. *Nat. Commun.* **2023**, *14*, 3524.
- Li, Q. L.; Liu, S. X.; Xu, M. F.; Pan, X. Q.; Li, N.; Zhu, J.; Zhu, X. L. Selenide-containing soluble polyimides: high refractive index and redox responsiveness. *Eur. Polym. J.* **2020**, *122*, 109358.
- Sato, Y.; Sobu, S.; Nakabayashi, K.; Samitsu, S.; Mori, H. Highly transparent benzothiazole-based block and random copolymers with high refractive indices by RAFT polymerization. *ACS Appl. Polym. Mater.* **2020**, *2*, 3205–3214.
- Yue, T. J.; Ren, B. H.; Zhang, W. J.; Lu, X. B.; Ren, W. M.;

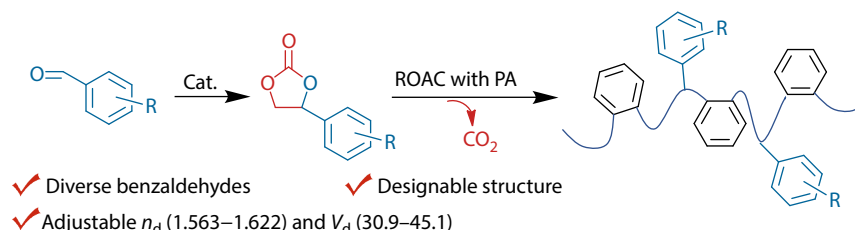
## Graphical Abstract

### Designable Optical Polyesters via Alternating Copolymerization of Benzaldehyde-derived Cyclic Carbonates and Phthalic Anhydride

Xue-Lin Song, Shun-Jie Liu, and Xian-Hong Wang

Changchun Institute of Applied Chemistry, Chinese Academy of Sciences; University of Science and Technology of China

This study presents a novel platform for designing aromatic polyesters with tunable optical properties. Benzaldehyde-derived cyclic carbonates were utilized to systematically control the polymer structure and optimize the optical performance through alternating copolymerization.



*Chinese J. Polym. Sci.*, 2026

<https://doi.org/10.1007/s10118-026-3630-9>

- Darensbourg, D. J. Randomly distributed sulfur atoms in the main chains of CO<sub>2</sub>-based polycarbonates: enhanced optical properties. *Angew. Chem. Int. Ed.* **2021**, *60*, 4315–4321.
- 13 Mavila, S.; Sinha, J.; Hu, Y. F.; Podgórski, M.; Shah, P. K.; Bowman, C. N. High refractive index photopolymers by thiol-yne "click" polymerization. *ACS Appl. Mater. Interfaces* **2021**, *13*, 15647–15658.
- 14 Zhang, C. J.; Hu, L. F.; Yang, J. L.; Cao, X. H.; Zhang, X. H. Alternating copolymerization of  $\gamma$ -selenobutyrolactone with episulfides for high refractive index selenium-containing polythioesters. *Eur. Polym. J.* **2020**, *133*, 109776.
- 15 Huo, N.; Rivkin, J.; Jia, R. B.; Zhao, Y. E.; Tenhaeff, W. E. Synthesis of high refractive index polymer thin films for soft, flexible optics through halomethane quaternization of poly(4-vinylpyridine). *Adv. Opt. Mater.* **2024**, *12*, 2302201.
- 16 Ryu, D.; Lee, M.; Sohn, H.; You, N. H. Synthesis and characterization of aromatic poly(phosphonate)s, poly(thiophosphonate)s, and poly(selenophosphonate)s for high refractive index. *Macromol. Res.* **2023**, *31*, 583–592.
- 17 You, H.; Wang, E. H.; Cao, H.; Zhuo, C. W.; Liu, S. J.; Wang, X. H.; Wang, F. S. From impossible to possible: atom-economic polymerization of low strain five-membered carbonates. *Angew. Chem. Int. Ed.* **2022**, *61*, e202113152.
- 18 You, H.; Yan, S.; Song, X. L.; Zhuo, C. W.; Liu, S. J.; Wang, X. H. Precise construction of polyester polyol from organocatalysis: epoxide slow-release and capture strategy. *Acta Polymerica Sinica* (in Chinese) **2023**, *54*, 327–335.
- 19 Kuang, Q. X.; Liu, S. J.; Liao, C.; Yang, L. H.; Cao, H.; Zhuo, C. W.; Pang, X.; Chen, X. S.; Wang, X. H. Swellable supported catalyst enables repeatable coupling of CO<sub>2</sub> and epoxides. *Sci. China Chem.* **2025**, *68*, 6551–6563.
- 20 Watanabe, S.; Cavinato, L. M.; Calvi, V.; van Rijn, R.; Costa, R. D.; Oyaizu, K. Polarizable H-bond concept in aromatic poly(thiourea)s: unprecedented high refractive index, transmittance, and degradability at force to enhance lighting efficiency. *Adv. Funct. Mater.* **2024**, *34*, 2404433.
- 21 Wang, Y. C.; Li, M. S.; Wang, S. X.; Tao, Y. H.; Wang, X. H. S-carboxyanhydrides: ultrafast and selective ring-opening polymerizations towards well-defined functionalized polythioesters. *Angew. Chem. Int. Ed.* **2021**, *60*, 10798–10805.
- 22 Zhang, K.; Ren, B. H.; Liu, X. F.; Wang, L. L.; Zhang, M.; Ren, W. M.; Lu, X. B.; Zhang, W. Z. Direct and selective electrocarboxylation of styrene oxides with CO<sub>2</sub> for accessing  $\alpha$ -hydroxy acids. *Angew. Chem. Int. Ed.* **2022**, *61*, e202207660.
- 23 Peña-López, M.; Neumann, H.; Beller, M. Iron-catalyzed synthesis of five-membered cyclic carbonates from vicinal diols: urea as sustainable carbonylation agent. *Eur. J. Org. Chem.* **2016**, *2016*, 3721–3727.
- 24 Honda, M.; Tamura, M.; Nakao, K.; Suzuki, K.; Nakagawa, Y.; Tomishige, K. Direct cyclic carbonate synthesis from CO<sub>2</sub> and diol over carboxylation/hydration cascade catalyst of CeO with 2-cyanopyridine. *ACS Catal.* **2014**, *4*, 1893–1896.
- 25 Abassian, M.; Zhiani, R.; Motavalizadehkakhky, A.; Eshghi, H.; Mehrzad, J. A new class of organoplatinum-based DFNS for the production of cyclic carbonates from olefins and CO<sub>2</sub>. *RSC Adv.* **2020**, *10*, 15044–15051.
- 26 Cheng, T. Y.; Wang, H. D.; Ding, J. Q.; Fang, J. G.; Wang, J.; Li, M. Z.; Chen, J.; Qin, A. J.; Tang, B. Z. Catalyst-free multicomponent polymerization of aldehydes, amines and trimethylsilyl cyanide toward poly( $\alpha$ -aminonitrile)s. *Polym. Chem.* **2024**, *15*, 2287–2295.
- 27 Li, H. B.; Fu, J.; Deng, F. Y.; Gui, Q.; Zhang, H. L. Efficient synthesis of high refractive index polymers containing diphenyl sulfone moieties with high optical transmittance and tunable Abbe number via free radical polymerization. *Eur. Polym. J.* **2026**, *242*, 114416.
- 28 Li, W. Z.; Ding, Y. L.; Gao, H.; Pan, L.; Li, Y. S. Design and synthesis of colorless cyclic olefin polymers with high refractive index, transparency, and thermal stability. *Macromolecules* **2025**, *58*, 9459–9468.
- 29 Zhang, X. Y.; Jones, G. O.; Hedrick, J. L.; Waymouth, R. M. Fast and selective ring-opening polymerizations by alkoxides and thioureas. *Nat. Chem.* **2016**, *8*, 1047–1053.
- 30 Liu, K. G.; Liu, S. J.; Fan, P. X.; Zhang, R. Y.; Chen, X. S.; Wang, X. H. Bifunctional porphyrin aluminum catalyzed copolymerization of carbon dioxide and long chain terminal epoxide. *Acta Polymerica Sinica* (in Chinese) **2025**, *56*, 242–252.
- 31 Fan, P. X.; Liu, S. J.; Zhang, R. Y.; Yang, L. H.; Gao, F. X.; Chen, X. S.; Wang, X. H. Flexible tethered binuclear porphyrin aluminum for the copolymerization of CO<sub>2</sub> and epoxide. *Acta Polymerica Sinica* (in Chinese) **2025**, *56*, 47–57.
- 32 Ota, I.; Suzuki, R.; Mizukami, Y.; Xia, X. C.; Tajima, K.; Yamamoto, T.; Li, F.; Isono, T.; Satoh, T. Organobase-catalyzed ring-opening copolymerization of cyclic anhydrides and oxetanes: establishment and application in block copolymer synthesis. *Macromolecules* **2024**, *57*, 3741–3750.
- 33 Tang, L.; Navarro, L. A.; Chilkoti, A.; Zauscher, S. High-molecular-weight polynucleotides by transferase-catalyzed living chain-growth polycondensation. *Angew. Chem. Int. Ed.* **2017**, *56*, 6778–6782.
- 34 Zhou, H.; Liu, S. J.; Chen, P.; Cao, H.; Zhuo, C. W.; Wang, X. H. Photothermal polymerization of epoxides and carbon dioxide catalyzed by polymeric aluminum porphyrin. *Acta Polymerica Sinica* (in Chinese) **2025**, *56*, 1954–1964.
- 35 Li, H.; Luo, H. T.; Zhao, J. P.; Zhang, G. Z. Well-defined and structurally diverse aromatic alternating polyesters synthesized by simple phosphazene catalysis. *Macromolecules* **2018**, *51*, 2247–2257.
- 36 Clamor, C.; Beament, J.; Wright, P. M.; Cattoz, B. N.; O'Reilly, R. K.; Dove, A. P. Ring-opening polymerisation of alkyl-substituted  $\epsilon$ -caprolactones: kinetic effects of substitution position. *Polym. Chem.* **2024**, *15*, 1227–1233.
- 37 Jiang, L. H.; Wu, Y.; Tian, X.; Xue, W. P.; Li, H. H.; Kang, X. H.; Li, B. Mechanistic Insights into the effects of ureas and monomers on the ring-opening alternating copolymerization of epoxides and anhydrides catalyzed by organic base/urea. *Polymers* **2024**, *16*, 978.
- 38 Min, J. K.; Jung, Y.; Ahn, J.; Lee, J. G.; Lee, J.; Ko, S. H. Recent advances in biodegradable green electronic materials and sensor applications. *Adv. Mater.* **2023**, *35*, 2211273.
- 39 Rosal, I.; Brignou, P.; Guillaume, S. M.; Carpentier, J. F.; Maron, L. DFT investigations on the ring-opening polymerization of substituted cyclic carbonates catalyzed by zinc- $\beta$ -diketiminato complexes. *Polym. Chem.* **2015**, *6*, 3336–3352.
- 40 Wang, J. Q.; Zhu, Y. N.; Li, M. S.; Wang, Y. C.; Wang, X. H.; Tao, Y. H. Tug-of-war between two distinct catalytic sites enables fast and selective ring-opening copolymerizations. *Angew. Chem. Int. Ed.* **2022**, *61*, e202208525.
- 41 Skupin, R.; Haufe, G. Regioselectivity of the ring opening of propene oxides bearing electron-withdrawing substituents at the methyl group with Olah's reagent. *J. Fluorine Chem.* **1998**, *92*, 157–165.
- 42 Liu, J. X.; Wu, Z. H.; Wang, J.; Wang, Z. P.; Sun, Y. L.; Zhang, Q. Q.; Nie, H. R.; Zhao, R. Y.; Guo, Z. W. High refractive index and excellent transparent polyarylates containing pendant groups and thiophene. *ACS Appl. Polym. Mater.* **2025**, *7*, 3904–3912.
- 43 You, N. H.; Higashihara, T.; Yasuo, S.; Ando, S.; Ueda, M. Synthesis of sulfur-containing poly(thioester)s with high refractive indices and high abbe numbers. *Polym. Chem.* **2010**, *1*, 480–484.
- 44 Hougham, G.; Tesoro, G.; Viehbeck, A. Influence of free volume change on the relative permittivity and refractive index in fluoropolyimides. *Macromolecules* **1996**, *29*, 3453–3456.